The Journal of Chemical Physics

Hydration mediated interfacial transitions on mixed hydrophobic/hydrophilic nanodroplet interfaces

Cite as: J. Chem. Phys. **149**, 234704 (2018); https://doi.org/10.1063/1.5035161
Submitted: 13 April 2018 . Accepted: 30 November 2018 . Published Online: 20 December 2018

Filip Kovacik, Halil I. Okur, Nikolay Smolentsev, Rüdiger Scheu, and Sylvie Roke

AIP Publishing

Hydration mediated interfacial transitions on mixed hydrophobic/hydrophilic nanodroplet interfaces

Filip Kovacik, Halil I. Okur, Nikolay Smolentsev, Rüdiger Scheu, and Sylvie Roke
Laboratory for fundamental BioPhotonics (LBP), Institute of Bioengineering (IBI), and Institute of Materials Science (IMX), School of Engineering (STI), and Lausanne Centre for Ultrafast Science (LACUS), École Polytechnique Fédérale de Lausanne (EPFL), CH-1015 Lausanne, Switzerland

(Received 13 April 2018; accepted 30 November 2018; published online 20 December 2018)

Interfacial phase transitions are of fundamental importance for climate, industry, and biological processes. In this work, we observe a hydration mediated surface transition in supercooled oil nanodroplets in aqueous solutions using second harmonic and sum frequency scattering techniques. Hexadecane nanodroplets dispersed in water freeze at a temperature of ∼15 °C below the melting point of the bulk alkane liquid. Addition of a trimethylammonium bromide (C_XTA^+) type surfactant with chain length equal to or longer than that of the alkane causes the bulk oil droplet freezing transition to be preceded by a structural interfacial transition that involves water, oil, and the surfactant. Upon cooling, the water loses some of its orientational order with respect to the surface normal, presumably by reorienting more parallel to the oil interface. This is followed by the surface oil and surfactant alkyl chains losing some of their flexibility, and this chain stretching induces alkyl chain ordering in the bulk of the alkane phase, which is then followed by the bulk transition occurring at a 3 °C lower temperature. This behavior is reminiscent of surface freezing observed in planar tertiary alkane/surfactant/water systems but differs distinctively in that it appears to be induced by the interfacial water and requires only a very small amount of surfactant. https://doi.org/10.1063/1.5035161

INTRODUCTION

Biological systems composed of membranes, proteins, polyelectrolytes, and sugars owe their special function to the interplay of charges, water, and hydrophobic moieties. The balance of these interactions is delicate, and is influenced by the size of the system. In eukaryotic cells, lipids are often purposely arranged asymmetrically across the bilayer, resulting in an imbalance of charge and hydration.[1–7] This arrangement provides an asymmetrical environment for controlling and triggering specific membrane enzymes and also plays an important role in membrane fusion and bending.[8] Proteins are composed of a carefully balanced combination of charged, hydrophobic, and hydrophilic groups, and this balance determines the folding/unfolding and activity.[9] Aside from the balance of the number of hydrophilic and hydrophobic groups,[10] the distribution of such groups also influences the structural properties of materials[11] as well as the size of the system. Nanoscale interfaces can display distinctly different behavior from extended ones with identical composition.[12–15] For instance, surface tension of the sodium dodecyl sulfate (SDS) covered planar interface substantially differs from that of a surfactant-stabilized nanodroplet surface composed of the same chemicals. Additionally, in a more recent study,[16] it was shown that the interfacial water structure is more ordered inside water droplets compared to planar water interfaces.

To further investigate this balance of interactions on the nanoscale, we studied temperature dependent interfacial transitions mediated by charges. To limit the complexity of the topic at hand, we investigated surface transitions on hexadecane oil droplets in water stabilized with a dilute monolayer of positively charged surfactants dodecyltrimethylammonium bromide ($C_{12}TA^+$), hexadecyltrimethylammonium bromide ($C_{16}TA^+$), and octadecyltrimethylammonium bromide ($C_{18}TA^+$) with different alkyl chain length, larger, identical, or smaller than the length of the oil. For this type of system, it is known that hexadecane tends to supercool by ∼15 °C due to the lack of crystallization cores in the extremely pure droplets.[17,18] It is also expected that when the freezing transition is suppressed, interfacial ordering transitions are not likely to occur as without a nucleation core, the alkyl chains remain at an essentially random conformation on the surface.[19,20] However, monitoring the orientational ordering of droplet interfacial water molecules along the surface normal with second harmonic scattering (SHS)[10,21,22] and the oil and surfactant interfacial conformation with sum frequency scattering (SFS),[23–26] we found that there is an interfacial ordering transition that appears to be initiated by the hydrating water around the dilute layers of surfactant molecules and involves the water, the oil molecules, and the surfactants. This type of transition that involves all molecular constituents shows how delicate the balance of interactions is at nanoscale system interfaces.

Note: This article is part of the Special Topic "Nonlinear Spectroscopy and Interfacial Structure and Dynamics" in J. Chem. Phys.

RESULTS

Bulk droplet behavior

We first investigated the behavior of the bulk liquid hexadecane phase of the nanodroplets. Hexadecane nanodroplets with a diameter of 180 nm and stabilized with 1 mM of $C_{12}TA^+$ (CMC = 14–16 mM), $C_{16}TA^+$ (CMC = 0.92–1 mM), and $C_{18}TA^+$ (CMC = 0.3 mM) were produced in D_2O by sonication.[14] This procedure resulted in the formation of nanoemulsions stabilized by dilute monolayers of surfactant with ~6.5 nm^2 of oil surface per surfactant molecule.[14]

Using dynamic light scattering (DLS), we recorded the linearly scattered intensity, to probe the liquid-solid phase transition temperature of hexadecane droplets in water.[27] The liquid-solid phase transition is accompanied by a change in refractive index, which results in a change in the linear light scattering intensity.[27,28] Figure 1 shows linear light scattering intensities as a function of temperature for 0.05 vol. % hexadecane-in-water nanoemulsions with $C_{16}TA^+$ (blue) and $C_{12}TA^+$ (red). The measurements were performed in a temperature cycle starting with cooling from 25 °C to 0 °C and subsequently heating back to 25 °C. The heating/cooling rate for all measurements in this work was 1 °C/10 min. For all tested samples, the intensity shows a plateau with a slight positive slope as the temperature gradually decreases from 25 °C to ~3 °C. Note that while the bulk hexadecane oil has a freezing temperature of 18 °C, the freezing of hexadecane nanodroplets occurred at 1.5 °C ± 0.5. Such a supercooling behavior is well known for ultrapure alkanes in small compartments.[17,18,29–32] In the heating part of the cycle, the linearly scattered light intensity remained at the level of solid particles until ~16.5 °C when it returned to the room temperature scattering value. Repeating the cycle three times resulted in the same hysteresis loop with matching transition temperatures. Additionally, our freezing and melting temperatures agree with values reported in Refs. 17 and 18. Bulk freezing of hexadecane nanodroplets is therefore independent of the charge and size of the surfactants. To probe interfacial transitions, we follow the temperature dependent orientational order of water with SHS and the surface oil and surfactants with SFS.

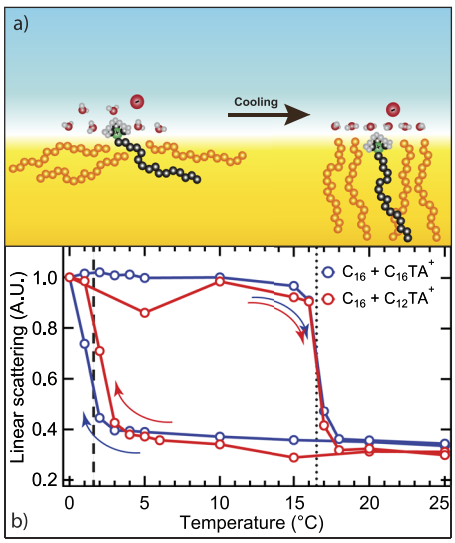

FIG. 1. **Schematic illustration of findings and bulk freezing of hexadecane oil-in-water nanodroplets**. (a) Schematic illustration of the findings of this work. The bulk solidification of the oil droplets is preceded by a surface transition, initiated by the water molecules that involve a larger number of in-plane oriented water molecules. This restructuring pushes the alkyl chains of the surfactants and alters the surface oil molecules, where they form a template for the bulk oil molecules to order around when the chain lengths match or when the alkyl chains of the surfactants are longer than those of the oil. (b) Linear light scattering for $C_{16}TA^+$ (blue) and $C_{12}TA^+$ (red) stabilized oil nanodroplets (diameter 180 nm) at a backscattering angle of 173° as a function of temperature. All measurements start at 25 °C first cooling the sample down to 0 °C and then heating it back up to 25 °C. The arrows indicate the direction of the cooling/heating process and the transitions observed in the light scattering intensity. The dashed line at 1.5 °C and dotted line at 16.5 °C indicate the freezing and melting transitions of hexadecane, respectively. Each sample consists of 0.05 vol. % hexadecane oil stabilized with 0.05 mM of surfactant dispersed in H_2O.

Interfacial transition

SFS is a vibrational coherent spectroscopy that measures the combined infrared and Raman spectrum of molecules in non-centrosymmetric environments, such as interfaces.[24,33] Due to the inherent sensitivity to non-centrosymmetry, the alkyl chain conformation of the interfacial molecules can be probed by the amplitude ratio of the symmetric (s)-CH_2 stretch (d^+) and the s-(CH_3) stretch (r^+) modes (d^+/r^+).[34,35] An all-trans alkyl chain conformation gives rise to $d^+/r^+ \ll 1$, whereas alkyl chain gauche defects result in $d^+/r^+ \geq 1$. Angle resolved SHS, on the other hand, is a non-resonant second-order nonlinear optical technique that has been utilized to probe the orientational ordering of interfacial water molecules along the surface normal.[10,36–39] Here, it is employed to probe phase transition induced changes in the orientational directionality of the water molecules along the surface normal as compared to bulk water.[40]

Figure 2 shows the SH intensity of surfactant stabilized nanoemulsions as a function of temperature. The employed surfactants included $C_{18}TA^+$ (red), $C_{16}TA^+$ (blue), and $C_{12}TA^+$

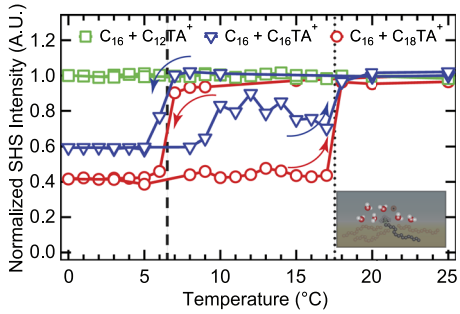

FIG. 2. **Water structure around hexadecane oil-in-water nanodroplets**. Normalized second harmonic scattering intensities for $C_{18}TA^+$ (red), $C_{16}TA^+$ (blue), and $C_{12}TA^+$ (green) stabilized oil nanodroplets (diameter 180 nm) measured at a 45° scattering angle as a function of temperature using the PPP polarization combination (that is, all beams polarized parallel to the horizontal scattering plane). All measurements start at 25 °C first cooling the sample down to 0 °C and then heating it back up to 25 °C. The arrows indicate the direction of the cooling/heating process and the transition in the SH scattering intensity. The dashed line at 6.5 °C and dotted line at 17.5 °C represent reordering of the interfacial water network. Each sample consists of 0.1 vol. % hexadecane stabilized with 0.1 mM of surfactant dispersed in H_2O. The inset displays an illustration of the interface with the probed water molecules in the forefront highlighted.

(green). The SHS intensity at each temperature was normalized with respect to the intensity of solutions that contain surfactants but no droplets. For the shorter-tailed $C_{12}TA^+$, the SHS intensity remains unaffected in the employed temperature region. The $C_{18}TA^+$ and $C_{16}TA^+$ stabilized nanodroplets generate a constant normalized SH intensity as they are cooled from 25 °C to 7 °C, after which it drops down at ~6.5 °C to 60% for $C_{18}TA^+$ and 40% for $C_{16}TA^+$ of their initial values at 25 °C. Such a decrease in the SHS intensity demonstrates a reduction in the orientational order of water at the interface. This decrease in orientational order relative to the surface normal occurs at ~5 °C higher temperatures than the bulk oil transition temperature. On the heating cycle, the SHS intensity remains at the lower level up to 17 °C for the longest alkyl chain, but varies between 9 °C and 17.5 °C for $C_{16}TA^+$. Finally, at ~18 °C, the bulk melting point of hexadecane, the SHS intensity returns to its original value indicating that the orientational order of water has increased again. Next, we performed sum frequency scattering to investigate interfacial phase transition of the oil hexadecane phase. Using the deuterated surfactant, we shifted the vibrational modes of the alkyl chain and head group outside of the probing window allowing us to probe just the interfacial oil alkyl chain conformation.

Figure 3(a) shows four SFS vibrational spectra in the C–H stretch region (2750–3050 cm^{-1}) of the interfacial oil molecules of droplets stabilized with d_{33}-$C_{16}TA^+$ at three different temperatures of the cooling cycle (red, blue, and black traces) and one of the heating cycle (green). The spectra were fitted using the symmetric CH_2 stretch mode (d^+, ~2855 cm^{-1}), the symmetric CH_3 stretch mode (r^+, at ~2877 cm^{-1}), the antisymmetric CH_2 stretch mode (d^-, at ~2920 cm^{-1}), the antisymmetric CH_3 stretch mode (r^-, at ~2965 cm^{-1}), the Fermi resonance of the symmetric CH_2 stretch mode (d^+_{FR}, at ~2905 cm^{-1}) and the Fermi resonance of the symmetric CH_3 stretch mode ($r^+_{FR,}$ ~2936 cm^{-1}).[19,41,42] The solid black lines represent fits to the spectra (see the supplementary material for a description and the fitted values). Figure 3(b) shows the amplitude ratio of the CH_2 symmetric stretch mode (d^+, ~2855 cm^{-1}) and the CH_3 symmetric stretch mode (r^+, ~2877 cm^{-1}), which is a measure of alkyl chain order. When the amplitude ratio $d^+/r^+ \rightarrow 0$, it means that the alkyl chains are in an all-trans conformation.[19,34,43] When the d^+ mode increases in amplitude relative to that of the r^+ mode, the alkyl chains exhibit more gauche defects.

Figure 3(b) thus displays the degree of ordering of the alkane alkyl chains at the nanodroplet/water interface. At the freezing temperature, a transition in the tail ordering occurs. Therefore, we can relate the d^+/r^+ ratio directly to the surface freezing of hexadecane.[28,42,44,45] The d^+/r^+ ratio maintains a value of 2.2 ± 0.2 when cooling from 25 °C to 6 °C and then starts to sharply decrease to reach a value of 0.6 ± 0.1 at 0 °C. The mid-point of this transition occurs at ~5 °C (dashed line). This interfacial transition temperature is slightly lower than the interfacial water transition temperature (6.5 °C) observed in Fig. 2. This suggests that the interfacial oil ordering and water ordering occur sequentially. Both interfacial transitions occur at least 3 °C above the bulk nanodroplet freezing temperature (Fig. 1). Upon heating, the d^+/r^+ ratio remains constant at 0.6 ± 0.1 between 0 °C and 10 °C, which is followed by a

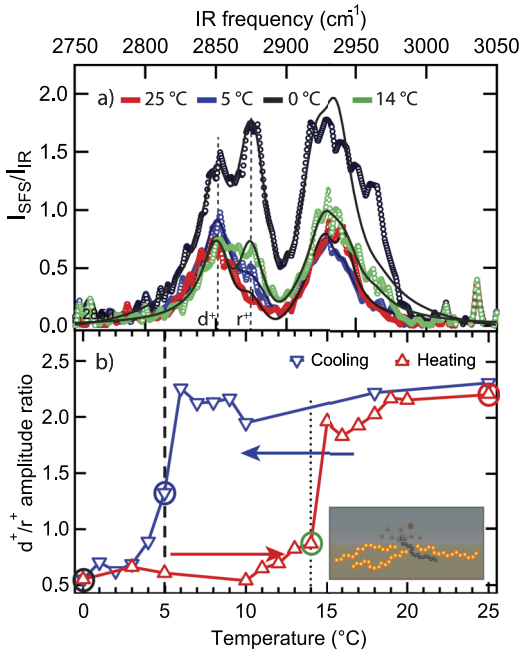

FIG. 3. **Oil surface structure of hexadecane oil-in-water nanodroplets**. (a) Figure shows the sum frequency scattering spectra from oil for $C_{16}TA^+$ stabilized oil nanodroplets (diameter ~180 nm) at the selected temperatures in the CH stretch vibrational region. The polarization combination used is SSP. (b) Figure shows the d^+/r^+ amplitude ratio as a function of temperature for the same sample. The measurement starts at 25 °C cooling the sample down to 0 °C and then heating it back up to 25 °C. The arrows indicate the direction of the cooling/heating process and the transition in the d^+/r^+ ratio. The dashed line at 5 °C and dotted line at 14 °C indicate surface melting and surface freezing of the nanodroplets. Each sample consists of 1 vol. % hexadecane oil stabilized with 1 mM d-$C_{16}TA^+$ in D_2O. Inset illustration with the probed hexadecane molecules in the forefront is included.

shallow transition over a wider temperature range starting at ~10 °C and ending at ~15 °C, where the d^+/r^+ ratio returned to 2.0 ± 0.2.

Next, we performed SFS experiments, now deuterating the oil phase and probing the alkyl chain conformation of the surfactants in the same spectral region. The vibrational modes of the head group vibrate at higher frequencies and are not recorded.[37] Figure 4 depicts the sum frequency spectra of the $C_{16}TA^+$ surfactant molecules as a function of temperature. This experiment is again aimed to investigate the relative amplitudes of the CH_2 symmetric stretch mode (d^+, ~2852 cm^{-1}) and CH_3 symmetric stretch mode (r^+, ~2875 cm^{-1}) originating from the non-deuterated $C_{16}TA^+$ and thus to determine the alkyl chain ordering of the surfactant as a function of temperature. The spectral features are comparable to those in Fig. 3(a), but the relative amplitudes vary. Four spectra of the alkyl tails of $C_{16}TA^+$ are plotted in Fig. 4(a). Black lines are fits to the data (the details of which can be found in the supplementary material), and the d^+/r^+ ratios are plotted as a function of temperature in Fig. 4(b). The d^+/r^+ of the $C_{16}TA^+$ alkyl chains was in the range of 1.0 ± 0.2 between 25 °C and 5 °C, which is lower than that of the interfacial hexadecane, indicating that the surfactant alkyl chains are more stretched with fewer gauche defects than the alkyl chains of the surface hexadecane molecules, as they have the same number of C atoms. Below 5 °C (midpoint 3 °C

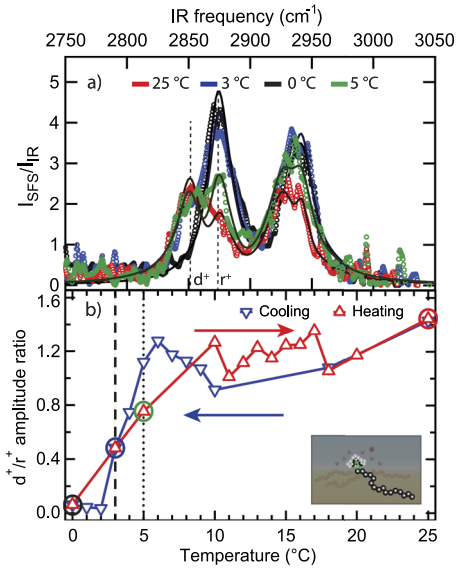

FIG. 4. **Surfactant surface structure in hexadecane oil-in-water nanodroplets**. (a) Figure shows the sum frequency scattering spectra in the SSP polarization combination from the surfactant molecules for the $C_{16}TA^+$ stabilized oil nanodroplets (diameter ~180 nm) at the selected temperatures in the CH spectral region. (b) Figure shows the d^+/r^+ amplitude ratio as a function of temperature for the same sample. The measurement starts at 25 °C cooling the sample down to 0 °C and then heating it back up to 25 °C. The arrows indicate the direction of the cooling/heating process and the transition in the d^+/r^+ ratio. The dashed line at 3 °C and dotted line at 5 °C indicate reorientation of surfactant chains and their return to original conformation, respectively. Each sample consists of 1 vol. % d-hexadecane oil stabilized with 1 mM $C_{16}TA^+$ in D_2O. Inset illustration with the probed surfactant molecules in the forefront is included.

indicated with the dashed line), the d^+/r^+ ratio drops to a value of 0.1 ± 0.1 at 2 °C. Upon heating, the alkyl chains do not display any hysteresis and identical average chain conformations are observed for cooling and heating. This is different from what was observed for the hydrating water and the oil interface.

DISCUSSION

Adding the structural information from Figs. 2–4, one possible explanation could be that the water molecules form a more in-plane orientation at the oil/water interface upon cooling. This type of structural transformation would be accompanied by restructuring of surface oil molecules and followed by repositioning of the "hydrophobic" trimethylammonium ions to be dissolved more into the interfacial oil phase.[10,46] This means that the complete alkyl chain will be dissolved in the oil phase, and in this position, it exhibits less gauche defects. These stretched alkyl chains of the surface oil molecules form a template for the surfactant molecules to become more ordered as well. When the system is heated, the process occurs in reverse. However, this time surfactant molecules initiate the disordering process. Then, the alkyl tails of the oil remain "locked" in the all-trans conformation until 15 °C, 3° below its macroscopic transition temperature, after which gauche defects reoccur and the surrounding water network returns to its original state.

Thus, for hydrophobic oil droplets stabilized with dilute monolayers of cationic surfactants, there is an interfacial structural transition when the surfactant alkyl chain is equal to or longer than the chain length of the oil phase. We also observe that the interfacial water layer changes its structure upon cooling at higher temperatures than the transitions observed in the alkyl chains of the surfactant and the oil phases. It therefore appears that the water drives the structural transformation.

Surface order transitions in the form of surface freezing have been investigated in planar alkane/air and alkane/water interfaces using X-ray scattering,[47–51] ellipsometry,[52,53] surface tension measurements,[54–58] and reflection sum frequency generation experiments.[42] The effect has been observed in alkanes with chain lengths between 16 and 50 carbons at the interface with air and, with the addition of a cationic surfactant ($C_{16}TA^+$), could also be induced at the alkane/water interface,[51,54,59,60] where it does not occur spontaneously. It has been shown experimentally[54,59] that for surfactant induced surface freezing at a planar alkane/water interface, the surfactant tail has to be strictly longer than the alkane chain length. The tetradecane/water/$C_{16}TA^+$ interface exhibits surface freezing, but the hexadecane/water/$C_{16}TA^+$ interface does not. The explanation for this behavior is that matching alkane and surfactant alkyl tails in length increases van der Waals interactions between the two species. The situation is similar if the surfactant tail is longer since van der Waals interactions are still maintained along the entire alkane tail. On the other hand, the disappearance of surface freezing is most likely of enthalpic origin.[59] Shorter surfactant tails leave molecular "voids" in the otherwise perfectly ordered surface monolayer which prevents the onset of surface freezing. It is also important to mention that entropy of mixing plays minimal role because the composition of the interface does not undergo significant changes at the phase transition.[59] This explanation requires the presence of a densely packed monolayer of alkyl chains and predicts[54] that when the system is altered such that the freezing transition is suppressed (by super cooling), this type of transition will not occur.

Considering our observations and the above conclusions drawn from planar interface experiments, it appears that important differences exist between the nanoscopic and macroscopic length scale. The observation that a surface transition occurs also on the interface of nanodroplets, despite also exhibiting supercooling, with a very dilute layer of surfactants suggests that additional interactions are relevant to the ones discussed above. In particular, since the water appears to initiate the surface ordering transformation, and the surfactant layer is dilute, the interaction of the charged head groups with water appears to be relevant.

These observations are in line with previous work that emphasizes the complexity of nanoscale systems compared to macroscopic systems. When system size becomes smaller, the balance of interactions becomes more complex with smaller discrepancies in the energy landscape. This has been observed experimentally on several occasions. For example, while planar extended interfaces with surfactants exhibit a significant (~40 mN/m) drop in surface tension, the nanoscopic equivalent exhibits a mere ~5 mN/m decrease when the sodium dodecyl sulfate concentration is varied over 3 orders of magnitude.[14] This type of difference can be explained by a shift

in the importance of electrostatic interactions that are relatively more important for the stability of nanoscale systems than macroscopic systems.[61] In addition, it has been observed that water droplets in a mixture of hydrophobic liquids display more ordering in their surface structures than extended planar interfaces,[16] suggesting that curvature is important for the formation of a more tetrahedrally ordered water network parallel to the interface. For the present study, both effects appear to be relevant.

CONCLUSIONS

In summary, we performed temperature dependent second harmonic, sum frequency, and linear light scattering measurements on alkane-in-water nanoemulsion systems. All emulsified systems exhibited supercooling of ~15 °C independent of the surfactant employed. Upon cooling, systems with C_XTA^+ surfactants longer or equal in tail length than the corresponding alkane first underwent a transformation in the interfacial water ordering. Subsequently, the surface layer of the droplets transformed into a more ordered one, where the surface oil and the surfactant tails achieve a more stretched conformation. Finally, the droplets solidified in their entirety. This observation suggests that the interfacial water structure plays a crucial role in the formation of the ordered "frozen" surface monolayer and potentially even induces the phenomenon. In the case of C_XTA^+ surfactants shorter than the alkane, such effects were not detected. These are important differences with the behavior at planar alkane/water interfaces where the surface transition can be explained involving only van der Waals interactions. That the hydration plays a crucial role and that surface ordering transitions can be induced by very dilute layers of surfactants point to the importance of length scales and the fact that the balance of interactions becomes more complex as soon as the length scale of the system is reduced.

MATERIALS AND METHODS

Chemicals

The oil phase employed included hydrogenated hexadecane (Sigma Aldrich, 99.8+%) and deuterated d_{34}-hexadecane (Cambridge Isotopes, 98%). Surfactants used included deuterated d_{25}-dodecyltrimethylammonium bromide (C_{12}TAB, Sigma Aldrich, 98%), hydrogenated dodecyltrimethylammonium bromide (C_{12}TAB, Sigma Aldrich, 98%), deuterated d_{33}-cetyltrimethylammonium bromide (C_{16}TAB, CDN Isotopes, 98%), hydrogenated cetyltrimethylammonium bromide (C_{16}TAB, Sigma Aldrich, 98%), and hydrogenated octadecyltrimethylammonium bromide (C_{18}TAB, Sigma Aldrich, 98%). All chemicals were used as received without further purification. Prior to use, glassware was cleaned using piranha solution consisting of a 3:1 ratio of H_2SO_4 (95%–97%, ISO, Merck) and H_2O_2 (Reactolab SA, 30%) and thoroughly rinsed with ultrapure water (H_2O, Milli-Q UF Plus, Millipore, Inc., electrical resistance of 18.2 MΩ cm) afterwards.

Droplet preparation and characterization

Droplets were prepared using an oil phase and D_2O (Armar Chemicals, 99.8+%) or ultrapure H_2O (Milli-Q UF Plus, Millipore, Inc., electrical resistance of 18.2 MΩ cm) as a solvent. In order to stabilize the oil droplets, one of the above mentioned surfactants was used in each case. The emulsions were prepared using a two-step process. First, hexadecane oil ($C_{16}H_{34}$, or $C_{16}D_{34}$), the desired surfactant, and the solvent were mixed for 2 min with a hand-held homogenizer (TH, OMNI International). A standard sample contains 1% v/v of oil and 1 mM of surfactant in H_2O (for SHS) or D_2O (for SFS). Second, an ultrasonication step was performed for 3–20 min (Bandelin 35 kHz, 400W). The nanodroplet size was measured using the dynamic light scattering technique (Malvern ZS nanosizer). A typical nanodroplet size distribution of a sample was ~180 nm in diameter with a polydispersity index (PDI) of ~0.15 (see S1 of the supplementary material for all the values). At 1% volume concentration of hexadecane and 1 mM of surfactant, the 180 nm in diameter droplets presented a total surface area of ~3000 cm^2/ml.[10]

Linear light scattering data were obtained using the Zetasizer Nano ZS (Malvern Instruments). The principal components of the setup are two laser sources (532 nm, max 50 mW and 633 nm, max 4 mW), a sample cell, and two light detectors (at 90° and 173°). Other components include a range of attenuating filters (transmission range from 0.0003% to 100%) in order to optimize the light intensity reaching the detector and a temperature controller of the sample cell (range from 0 to 90 °C ± 0.1). During each measurement, a suitable laser beam was introduced into the cell and the scattered light was collected at 173°. Traditionally, the signal obtained from the scattered light is fed into a multi-channel correlator that generates a function used to determine the translational diffusion coefficient of the particles analyzed. The Stokes-Einstein equation is then used to calculate the particle size. However, we utilized the changes in raw intensity of light backscattered from our sample to observe phase transitions of the sample.[28]

Vibrational sum frequency spectra were measured using the setup for sum frequency generation experiments described in Refs. 46, 62, and 63. An 800 nm regeneratively amplified Ti:sapphire system (Spitfire Pro, Spectra physics) seeded with an 80 MHz 800 nm oscillator (Integral 50, Femtolasers) was operated at a 1 kHz repetition rate to pump a commercial OPG/OPA/DPG system (HE-TOPAS-C, Light Conversion), which was used to generate IR pulses. The visible beam was split off directly from the amplifier and spectrally shaped with a home-built pulse shaper. The angle between the 10 μJ visible (VIS) beam (800 nm, FWHM 15 cm^{-1}) and the 6 μJ IR beam (9700 nm or 3200 nm, FWHM 160 cm^{-1}) was 20° (as measured in air). The focused laser beams were overlapped in a sample cuvette with a path length of 200 μm. The sample cuvette was placed in a custom built Peltier cooled holder from Quantum Northwest with a 0.1° temperature control accuracy. At a scattering angle of 55°, the scattered SF light was collimated using a plano-convex lens (f = 15 mm, Thorlabs LA1540-B) and passed through two short pass filters (3rd Millenium, 3RD770SP). The SF light was spectrally dispersed with a monochromator (Acton, SpectraPro 2300i) and detected with an intensified CCD camera (Princeton Instruments, PI-Max3) using a gate width of 10 ns. The acquisition time for a single spectrum was 150 s.

A Glan-Taylor prism (Thorlabs, GT15-B), a half-wave plate (EKSMA, 460-4215), and a polarizing beam splitter cube (CVI, PBS-800-050) and two BaF_2 wire grid polarizers (Thorlabs, WP25H-B) were used to control the polarization of the Sum Frequency (SF), VIS, and IR beams, respectively. The SF and VIS beams were polarized in the vertical (S) direction, and the IR beam was polarized in the horizontal plane (P), leading to the polarization combination $S_{out}S_{in}P_{in}$. The recorded intensity was baseline subtracted and normalized to the SF spectrum of $KNbO_3$ nanoparticles in $P_{out}P_{in}P_{in}$ polarization that was recorded before each measurement. Information about SFS spectral fitting can be found in S2 of the supplementary material.

Second harmonic scattering measurements were performed using 190 fs laser pulses at 1028 nm with a 200 kHz repetition rate. The input polarization is controlled by a Glan-Taylor polarizer (GT10-B, Thorlabs) and a zero-order half-wave plate (WPH05M-1030). The filtered (FEL0750, Thorlabs) input pulses with a pulse energy of 0.3 μJ (incident laser power P = 60 mW) were focused into a cylindrical glass sample cell (4.2 mm inner diameter) with a waist diameter of ~32 μm and a Rayleigh length of 3.2 mm. The sample cuvette was placed in a custom built Peltier cooled holder from Quantum Northwest with a 0.1° temperature control accuracy. The scattered SH light was collected and collimated with a plano-convex lens (f = 5 cm), polarization analyzed (GT10-A, Thorlabs), filtered, (ET525/50, Chroma), and finally focused into a gated photomultiplier tube (PMT, H7421-40, Hamamatsu). Data points for single angle measurements were acquired at the θ = 45° angle of the detector arm and an acceptance angle of 11.4°. Typically, measurement settings were 20 × 1.5 s acquisition time and a gate width of 10 ns. To correct for incoherent hyper Rayleigh scattering from the aqueous phase, both the SHS response from the oil droplet solution and the SHS response from the solution without oil droplets are detected under the same conditions. The SHS intensity from the solution is then subtracted from the SHS intensity from the oil droplet emulsion. The obtained difference is then normalized to the isotropic SSS signal of pure water so that we correct for any form of aberration due to differences in the beam profile and obtain a value that can be compared to any other measurement done in the same procedure. The normalization procedure is summarized by the following equation:

$$S_{PPP}(\theta) = \frac{I_{EMULSION,PPP}(\theta) - I_{SOLUTION,PPP}(\theta)}{I_{WATER,SSS}(\theta)}. \quad (1)$$

SUPPLEMENTARY MATERIAL

See supplementary material for sections of the size distribution and PDI of nanodroplets (S1) and SFG spectral fitting (S2) as well as Tables S1–S3.

ACKNOWLEDGMENTS

This work was supported by the Julia Jacobi Foundation, the Swiss National Science Foundation (Grant No. 200021_140472), and the European Research Council (Grant Nos. 240556 and 616305).

[1] K. L. Brown and J. C. Conboy, J. Am. Chem. Soc. **133**, 8794–8797 (2011).
[2] D. L. Daleke, J. Biol. Chem. **282**, 821–825 (2007).
[3] G. Lenoir, P. Williamson, and J. C. M. Holthuis, Curr. Opin. Chem. Biol. **11**, 654–661 (2007).
[4] T. Pomorski, J. C. M. Holthuis, A. Herrmann, and G. van Meer, J. Cell Sci. **117**, 805 (2004).
[5] G. van Meer, D. R. Voelker, and G. W. Feigenson, Nat. Rev. Mol. Cell Biol. **9**, 112–124 (2008).
[6] A. A. Gurtovenko and I. Vattulainen, J. Phys. Chem. B **112**, 4629–4634 (2008).
[7] N. Smolentsev, C. Lütgebaucks, H. I. Okur, A. G. F. de Beer, and S. Roke, J. Am. Chem. Soc. **138**, 4053–4060 (2016).
[8] P. F. Devaux, Annu. Rev. Biophys. Biomol. Struct. **21**, 417–439 (1992).
[9] B. Alberts, A. Johnson, J. Lewis, M. Raff, K. Roberts, and P. Walter, *Molecular Biology of the Cell*, 4th edition (Garland Science, New York, 2002), p. 341.
[10] R. Scheu, Y. Chen, H. B. de Aguiar, B. M. Rankin, D. Ben-Amotz, and S. Roke, J. Am. Chem. Soc. **136**, 2040–2047 (2014).
[11] A. Walther and A. H. E. Müller, Chem. Rev. **113**, 5194–5261 (2013).
[12] S. Roke, ChemPhysChem **10**, 1380–1388 (2009).
[13] S. Roke, W. G. Roeterdink, J. E. G. J. Wijnhoven, A. V. Petukhov, A. W. Kleyn, and M. Bonn, Phys. Rev. Lett. **91**, 258302 (2003).
[14] H. B. d. Aguiar, A. G. F. de Beer, M. L. Strader, and S. Roke, J. Am. Chem. Soc. **132**, 2122–2123 (2010).
[15] H. B. de Aguiar, M. L. Strader, A. G. F. de Beer, and S. Roke, J. Phys. Chem. B **115**, 2970–2978 (2011).
[16] N. Smolentsev, W. J. Smit, H. J. Bakker, and S. Roke, Nat. Commun. **8**, 15548 (2017).
[17] E. Dickinson, D. J. McClements, and M. J. W. Povey, J. Colloid Interface Sci. **142**, 103–110 (1991).
[18] H. Kraack, E. B. Sirota, and M. Deutsch, J. Chem. Phys. **112**, 6873–6885 (2000).
[19] A. G. Lambert, P. B. Davies, and D. J. Neivandt, Appl. Spectrosc. Rev. **40**, 103–145 (2005).
[20] M. L. Schlossman and A. M. Tikhonov, Annu. Rev. Phys. Chem. **59**, 153–177 (2008).
[21] K. C. Jena, R. Scheu, and S. Roke, Angew. Chem., Int. Ed. **51**, 12938–12940 (2012).
[22] C. Sauerbeck, B. Braunschweig, and W. Peukert, J. Phys. Chem. C **118**, 10033–10042 (2014).
[23] J. H. Hunt, P. Guyot-Sionnest, and Y. R. Shen, Chem. Phys. Lett. **133**, 189–192 (1987).
[24] A. L. Harris, C. E. D. Chidsey, N. J. Levinos, and D. N. Loiacono, Chem. Phys. Lett. **141**, 350–356 (1987).
[25] E. C. Y. Yan, Z. Wang, and L. Fu, J. Phys. Chem. B **119**, 2769–2785 (2015).
[26] C. M. Johnson and S. Baldelli, Chem. Rev. **114**, 8416–8446 (2014).
[27] A. F. Behof, R. A. Koza, L. E. Lach, and P. N. Yi, Biophys. J. **22**, 37–48 (1978).
[28] S. Roke, J. Buitenhuis, J. C. V. Miltenburg, M. Bonn, and A. V. Blaaderen, J. Phys.: Condens. Matter **17**, S3469–S3479 (2005).
[29] E. Dickinson, F.-J. Kruizenga, M. J. W. Povey, and M. van der Molen, Colloids Surf., A **81**, 273–279 (1993).
[30] H. Kraack, M. Deutsch, and E. B. Sirota, Macromolecules **33**, 6174–6184 (2000).
[31] S. A. Vanapalli, J. Palanuwech, and J. N. Coupland, Colloids Surf., A **204**, 227–237 (2002).
[32] K. Jiang, Y. Su, B. Xie, S. Jiang, Y. Zhao, and D. Wang, J. Phys. Chem. B **112**, 16485–16489 (2008).
[33] Y. R. Shen, Nature **337**, 519–525 (1989).
[34] E. Tyrode and J. Hedberg, J. Phys. Chem. C **116**, 1080–1091 (2012).
[35] P. Guyot-Sionnest, J. H. Hunt, and Y. R. Shen, Phys. Rev. Lett. **59**, 1597–1600 (1987).
[36] S. Roke and G. Gonella, Annu. Rev. Phys. Chem. **63**, 353–378 (2012).
[37] R. Scheu, B. M. Rankin, Y. Chen, K. C. Jena, D. Ben-Amotz, and S. Roke, Angew. Chem., Int. Ed. **53**, 9560–9563 (2014).

[38]S. Ong, X. Zhao, and K. B. Eisenthal, Chem. Phys. Lett. **191**, 327–335 (1992).
[39]B. Schürer, S. Wunderlich, C. Sauerbeck, U. Peschel, and W. Peukert, Phys. Rev. B **82**, 241404 (2010).
[40]Y. Chen, K. C. Jena, C. Lütgebaucks, H. I. Okur, and S. Roke, Nano Lett. **15**, 5558–5563 (2015).
[41]R. A. MacPhail, H. L. Strauss, R. G. Snyder, and C. A. Elliger, J. Phys. Chem. **88**, 334–341 (1984).
[42]G. A. Sefler, Q. Du, P. B. Miranda, and Y. R. Shen, Chem. Phys. Lett. **235**, 347–354 (1995).
[43]E. Tyrode and J. F. D. Liljeblad, J. Phys. Chem. C **117**, 1780–1790 (2013).
[44]K. M. Wilkinson, L. Qunfang, and C. D. Bain, Soft Matter **2**, 66 (2006).
[45]D. Levy and K. A. Briggman, Langmuir **23**, 7155–7161 (2007).
[46]R. Scheu, Y. Chen, M. Subinya, and S. Roke, J. Am. Chem. Soc. **135**, 19330–19335 (2013).
[47]A. B. Herhold, D. Ertaş, A. J. Levine, and H. E. King, Phys. Rev. E **59**, 6946–6955 (1999).
[48]A. B. Herhold, H. E. King, and E. B. Sirota, J. Chem. Phys. **116**, 9036–9050 (2002).
[49]Y. Shinohara, N. Kawasaki, S. Ueno, I. Kobayashi, M. Nakajima, and Y. Amemiya, Phys. Rev. Lett. **94**, 097801 (2005).
[50]Y. Shinohara, T. Takamizawa, S. Ueno, K. Sato, I. Kobayashi, M. Nakajima, and Y. Amemiya, Cryst. Growth Des. **8**, 3123–3126 (2008).
[51]X. Z. Wu, B. M. Ocko, E. B. Sirota, S. K. Sinha, and M. Deutsch, Physica A **200**, 751–758 (1993).
[52]T. Pfohl, D. Beaglehole, and H. Riegler, Chem. Phys. Lett. **260**, 82–86 (1996).
[53]B. M. Ocko, X. Z. Wu, E. B. Sirota, S. K. Sinha, O. Gang, and M. Deutsch, Phys. Rev. E **55**, 3164–3182 (1997).
[54]E. Sloutskin, C. D. Bain, B. M. Ocko, and M. Deutsch, Faraday discuss. **129**, 339–352 (2005); discussion 353–366.
[55]E. Sloutskin, O. Gang, H. Kraack, A. Doerr, E. B. Sirota, B. M. Ocko, and M. Deutsch, Physical Rev. E **68**, 031606 (2003).
[56]E. Sloutskin, Z. Sapir, C. D. Bain, Q. Lei, K. M. Wilkinson, L. Tamam, M. Deutsch, and B. M. Ocko, Phys. Rev. Lett. **99**, 136102 (2007).
[57]E. Sloutskin, X. Z. Wu, T. B. Peterson, O. Gang, B. M. Ocko, E. B. Sirota, and M. Deutsch, Physical Rev. E **68**, 031605 (2003).
[58]E. B. Sirota, H. E. King, Jr., H. H. Shao, and D. M. Singer, J. Phys. Chem. **99**, 798–804 (1995).
[59]Q. Lei and C. D. Bain, Phys. Rev. Lett. **92**, 176103 (2004).
[60]L. Tamam, D. Pontoni, Z. Sapir, S. Yefet, E. Sloutskin, B. M. Ocko, H. Reichert, and M. Deutsch, Proc. Natl. Acad. Sci. U. S. A. **108**, 5522–5525 (2011).
[61]E. Zdrali, Y. Chen, H. I. Okur, D. M. Wilkins, and S. Roke, ACS Nano **11**, 12111–12120 (2017).
[62]H. B. de Aguiar, J.-S. Samson, and S. Roke, Chem. Phys. Lett. **512**, 76–80 (2011).
[63]H. B. de Aguiar, R. Scheu, K. C. Jena, A. G. F. de Beer, and S. Roke, Phys. Chem. Chem. Phys. **14**, 6826 (2012).